Research Article

SCI

Received: 24 April 2012 Revised: 11 June 2012 Accepted: 13 June 2012 Published online in Wiley Online Library: 20 July 2012

(wileyonlinelibrary.com) DOI 10.1002/jctb.3889

Assessment of aged biodegradable polymer-coated nano-zero-valent iron for degradation of hexahydro-1,3,5-trinitro-1,3,5-triazine (RDX)

Ru Xiao and Mahmoud Wazne*

Abstract

BACKGROUND: This study reports on the effects of aging on suspension behavior of biodegradable polymer-coated nano-zero-valent iron (nZVI) and its degradation rates of hexahydro-1,3,5-trinitro-1,3,5-triazine (RDX) under reductive conditions. The polymers investigated included guar gum, potato starch, alginic acid (AA), and carboxymethyl cellulose (CMC). Polymer coating was used to mitigate nZVI delivery hindrance for *in situ* treatment of RDX-contaminated groundwater.

RESULTS: The RDX degradation rates by bare nZVI and starch-coated nZVI suspensions were least affected by aging although these suspensions exhibited the least favorable dispersion behavior. CMC, AA, and guar gum coating improved nZVI rates of degradation of RDX but these rates decreased upon aging. The best suspension stability upon aging was achieved by CMC and AA. Guar gum with loadings rates one order of magnitude lower than that of CMC and AA achieved good iron stabilization but significantly higher RDX degradation rates.

CONCLUSION: It is demonstrated that both migration and reactivity of polymer-stabilized nZVI should be explicitly evaluated over a long period before application in the field. Guar gum coated nZVI appeared best suited for *in situ* application because it maintained good suspension stability, with RDX degradation rates least affected by aging compared with the other polymers tested.

Keywords: RDX degradation; suspension stability; iron nanoparticles; polymer-coated particles; biodegradable polymer

INTRODUCTION

Hexahydro-1,3,5-trinitro-1,3,5-triazine (CAS Reg. No. 121-82-4), commonly known as RDX or cyclonite is extensively used in military munitions formulations. According to US EPA, RDX was assigned to weight-of-evidence Group C, possible human carcinogen, exerting its primary toxic effect on the central nervous system (CNS).[1] RDX can enter the aquatic environment through industrial wastewater discharge or leaching from contaminated soils in the manufacturing areas or conflict theaters.

Several treatment processes including heated alkaline hydrolysis, ozonation, ultraviolet irradiation, photodegradation, and biodegradation have shown high RDX removal rates in aqueous solutions (first-order constant is about 10^{-1} s^{-1} and 10^{-2} s^{-1}); however, many of these technologies face limitations especially for *in situ* application.[2,3] Nano-zero-valent iron (nZVI) exhibits high reactivity towards organics and heavy metals and has a great potential for *ex situ* and *in situ* treatment of RDX.[4–6] Compared with the techniques mentioned above, nZVI is potentially an easier material to handle and apply.[7,8] RDX is reportedly degraded by ZVI via two routes. The first route involves denitration of RDX to produce intermediates like methylenedinitramine (MEDINA), MNX hexahydro-1-nitroso-,3,5-dinitro-1,3,5-triazine), DNX (hexahydro-1,3-dinitroso-5-nitro-1,3,5-triazine), and TNX (hexahydro-1,3,5-trinitroso-1,3,5-triazine). The second route involves reduction of the N-NO_2 functional groups to produce N-nitroso derivatives (MNX, DNX, and TNX).[9] Upon complete degradation of RDX, the formed products include NO_2^-, N_2, NH_3, N_2O, $HCOO^-$ and CH_2O.[10,11]

In situ treatment of RDX-contaminated groundwater is hindered by effective delivery of nZVI suspension to the contaminated plumes due to its rapid aggregation and deposition in the subsurface. Investigations of iron suspension stability and mobility have been carried out using anionic copolymer,[12] anionic carbon[13,14] and block polymer.[15] The simple electrostatic or long-ranged steric repulsion forces required to maintain stable suspensions are often achieved by high molecular weight polymers.[12] Polymer coating also improves the efficiency of the iron nanoparticles by controlling the crystal growth and formation of a greater number of reactive sites. The formation

* *Correspondence to: Mahmoud Wazne, W.M. Keck Geoenvironmental Laboratory, Center for Environmental Systems, Stevens Institute of Technology, Castle Point on Hudson, Hoboken, New Jersy 07030, USA.*
E-mail: mwazne@stevens.edu

W.M. Keck Geoenvironmental Laboratory, Center for Environmental Systems, Stevens Institute of Technology, Castle Point on Hudson, Hoboken, New Jersey 07030, USA

of larger reactive sites in combination with smaller size particles thereafter, improves the iron metal contact with contaminant ions.[9]

Ideally, modified nZVI nanoparticles should be inexpensive, simple to use, and have no adverse impact on the environment. Our choice of surface modifiers was mindful of the implications that rest beyond the simple engineering requirement for iron nanoparticle stabilization. The objective of this study was to assess the application of inexpensive, commercially available polymers for use as stabilizing agents and surface modifiers for iron nanoparticles. To achieve these aims, economic biodegradable polymers like alginic acid (AA), guar gum,[16] carboxymethyl cellulose (CMC),[5,8,9] and potato starch[17] were assessed for their effectiveness for nZVI stabilization and RDX reduction.

These polymers are widely used as emulsion stabilizers and thickeners in the food and drug industry due to their high viscosity. In the environmental field, carboxymethyl cellulose (CMC) is a cellulose derivative with carboxymethyl groups bound to some of the hydroxyl groups of the glucopyranose monomers that make up the cellulose backbone. CMC molecules, often used in the form of a sodium salt, are on average shorter than cellulose, have high cold water solubility, and are mainly used to control viscosity without gelling in foods.[18] Alginate is an unbranched block copolymer polysaccharide that comprises 1,4-linked â-D-mannuronic acid and R-L-guluronic acid residues. Guar gum is known for its extraordinary rheological properties attributed to the galactomannan structure having galactose and mannose in the molar ratio 1: 2. Guar gum does not have functional groups susceptible to changes in pH and ionic strength and therefore it is regarded as a strong potential coating material to modify the surface of nZVI.[16,19] Starch is made up of two fractions: amylose made up of essentially a-(1/4) D-glucopyranosyl units, and amylopectin made up of a large number of short chains.[20] It is reported to form complexes with Fe ions resulting in smaller nZVI particle size during synthesis.[21]

Freshly polymer-modified nZVI were reported to have high efficiency in removing RDX in aqueous media.[9,22–24] However, to the best of our knowledge, the long-term assessment of modified iron nanoparticle reactivity and suspension stability upon aging is lacking. In this study, freshly prepared nZVI and stabilized nZVI were preserved under anoxic conditions up to 4 weeks. The aged samples were used in RDX degradation tests and suspension stability experiments.

MATERIALS AND METHODS

Chemicals

Hexahydro-1,3,5-trinitro-1,3,5-triazine (RDX) was synthesized and supplied by the US Army TACOM/ARDEC (Picatinny, Arsenal, NJ). It had an Octahydro-1,3,5,7-tetranitro-1,3,5,7-tetrazocine (HMX) content of 10% (w/w) as a production related impurity. Ferrous sulfate ($FeSO4 \cdot 4H_2O$) was obtained from Fisher Scientific (Pittsburgh, PA). Alginic acid sodium salt (MW = 12 000–80 000g mol^{-1}), guar gum (MW = 220 000 g mol^{-1}), water soluble starch (MW = 342.3 g mol^{-1}) and carboxymethyl cellulose sodium salt (CMC MW = 250 000 g mol^{-1}) were obtained from Sigma-Aldrich (St Louis, MO). Sodium borohydride ($NaBH_4$) was obtained from Acros Organics (Geel, Belgium). Nitrogen gas (N_2) was obtained from Welding Supply Co. Inc. (NJ). Teflon syringe filters (0.2 µm) was purchased from Fisher Scientific (Pittsburgh, PA).

Preparation of iron nanoparticles

The synthesis of nanoscale iron particles was conducted using the aqueous phase reduction method. In brief, the preparation was carried out in a 1000 mL beaker attached to a nitrogen gas tube. In a typical preparation, 40 mL freshly prepared stock solution of ferrous sulfate hexahydrate ($FeSO_4 \cdot 4H_2O$) was added to 400 mL of deionized water, resulting in the desired concentration of iron solution. The mixture was then sparged with N_2 for 30 min to remove dissolved oxygen (DO). nZVI was synthesized by the addition of 40 mL $NaBH_4$ aqueous solution dropwise to the $FeSO_4$ aqueous solution at a rate of 0.0667 mL s^{-1}. The mixture was vigorously stirred by a vertical propeller in a nitrogen atmosphere. The final ZVI concentration was 0.2 g L^{-1}. After titration, the reactor was continuously sparged with nitrogen gas for 10 min to remove any residual hydrogen gas. Then, the Fe nanoparticle suspension was distributed into sample vials and stored in a glove box (LABCONCO) filled with nitrogen gas for later use in RDX degradation experiments, suspension stability experiments, or Zeta potential measurements.

The polymer coated nZVI was synthesized by titrating the borohydride solution into a beaker containing the ferrous sulfate solution pre-mixed with the designated polymer. Prior to titrating the borohydride into the polymer-ferrous mixture, the pure polymer solutions were individually homogenized overnight using magnetic stirrers.

Batch experiments

In this study, two polymer concentrations were used at 1% and 0.1%, except for guar gum where only one concentration at 0.1% was used due to difficulties with the synthesis and the HPLC analysis at high guar polymer concentration. Polymer concentrations are reported based on initial polymer weight percent added. Bare or modified nZVI solutions were prepared and introduced to 45mL clear glass vials with teflon septum caps. Bottles were capped and covered with aluminum foil to eliminate photodegradation of RDX. The degradation experiments were initiated by injecting 0.45 mL of RDX stock solution (4 g L^{-1} RDX in acetonitrile) into the nanoparticle suspensions vials, which were stored under oxygen-free conditions, resulting in an initial RDX concentration of about 40 mg L^{-1}. The prepared glass vials were then placed on an end-over-end rotator for set mixing intervals (10, 20, 30, 50, 80, 120, and 180 min) at room temperature of 25 °C. At each sampling time, 1 mL sub-samples were withdrawn and purged with oxygen for 1 min to stop the reaction. Samples were then centrifuged and filtered through 0.2 µm teflon filters before HPLC analysis. Control experiments indicated that the oxygen purging step had no effects on RDX content. All experiments were run in duplicate.

Transmission electron microscopy

An aliquot of 0.2 g L^{-1} bare iron and polymer modified iron nanoparticles suspension were subjected to TEM analysis using Phillips CM20 FEG STEM equipped with a Gatan 776 ENFINA spectrometer and an Emispec control and acquisition system. The TEM images were taken using a carbon support copper film substrate 400 mesh (Electron Microscopy Sciences, Hatfield, PA). One drop of the nanoparticle suspension was placed on the substrate in a dust-free environment for 5 min. As soon as the nanoparticles were attached to the substrate, a piece of filter paper was placed at the edge of the carbon substrate in touch with the suspension draining the remaining solution.

Zeta potential measurements

The zeta potential of the iron suspensions was measured using a Nano Zetasizer (Malvern, Worcestershire, UK). Briefly, 1 mL of the suspension was introduced into a disposable capillary cuvette (Sarstedt, Germany) to conduct the ζ-potential measurement. All DLS measurements were conducted at 25 °C. The Helmholtz–Smoluchowski relationship was used by the DTS Nano software to convert the measured electrophoretic mobilities to ζ-potential.[25]

UV-VIS measurements

The UV-VIS spectra of various iron–polymer combinations were monitored using a Diode Array Spectrophotometer (hp Hewlett Packard 8452A). The UV-VIS spectra of pure ferrous sulfate solution (0.2 g L^{-1}) and pure polymer solution (1%) were prepared and used as controls. A ferrous sulfate–polymer solution was prepared by mixing 1% of polymer with ferrous sulfate solution to attain a Fe^{2+} final concentration of 0.2 g L^{-1}. The ferrous–polymer solution was also used as control. 1 mL of the above control samples and various fresh and aged iron suspensions were filtered and examined by the spectrophotometer. The solution and suspensions were filtered using 0.2 µm syringe filters and were then scanned by the hp spectrophotometer within the wavelength range 190 nm to 800 nm.

Analytical

RDX was quantified by a high performance liquid chromatography (HPLC) instrument (Varian 920 Liquid Chromatograph) using an Adsorbosphere C18 10 µm 4.6 × 250 mm column with pre-filter and guard column (Alltech Adsorbosphere C18 5 µm). The HPLC instrument is equipped with a photodiode array (PDA) detector. The mobile phase comprised of water and methanol at 1 : 1, using an elution time of 10 min. The flow rate was kept constant at 1 mL min^{-1} and the spectrophotometric detection was obtained at 254 nm. The retention time of RDX was 5.5 min.

RESULTS AND DISCUSSION

Particle characterization

Representative TEM images of fresh and aged bare iron nanoparticles, starch, guar, alginate and CMC modified nZVI particles are shown in Fig. 1. The fresh bare iron nanoparticles appear round and aggregated with wide particle size distribution ranging approximately between 70 nm and 350 nm. No significant change was observed upon aging of the iron sample under anoxic conditions after 4 weeks. The fresh starch coated nZVI particles appear round with particle size of about 50 nm. The fine size distribution of the starch coated particles is most likely due to the formation of weak Fe^{2+}–starch complexes during synthesis, which hindered iron particle growth.[21] The particle size distribution appears close to the size distribution reported for starched iron particles ranging between 4 nm and 60 nm.[17] Some of the starch coated iron particles appear enclosed in a thick film of polymer forming clusters. Upon aging, the starch coated nZVI particles appear enclosed in larger clusters with some dispersed single particles. It is very difficult to determine the particles size of the iron particles enclosed in the clusters, but the size of singular particles appears similar to the ones in the fresh suspensions. Conversely, the fresh CMC coated nZVI particles appear very well dispersed with particle size in the order of few nanometers enmeshed in a homogeneous and continuous thin polymer film. These measurements were in agreement with those found in the literature. For example, Ghinwa Naja reported an average diameter size of 15 ± 4 nm when using CMC to coat reactive nano-iron particles (RNIP, nZVI with a Fe^0 core and Fe_3O_4 outer shell).[9] There was no significant change in particle size of the CMC coated nZVI particles upon aging for 4 weeks, but the particles appear

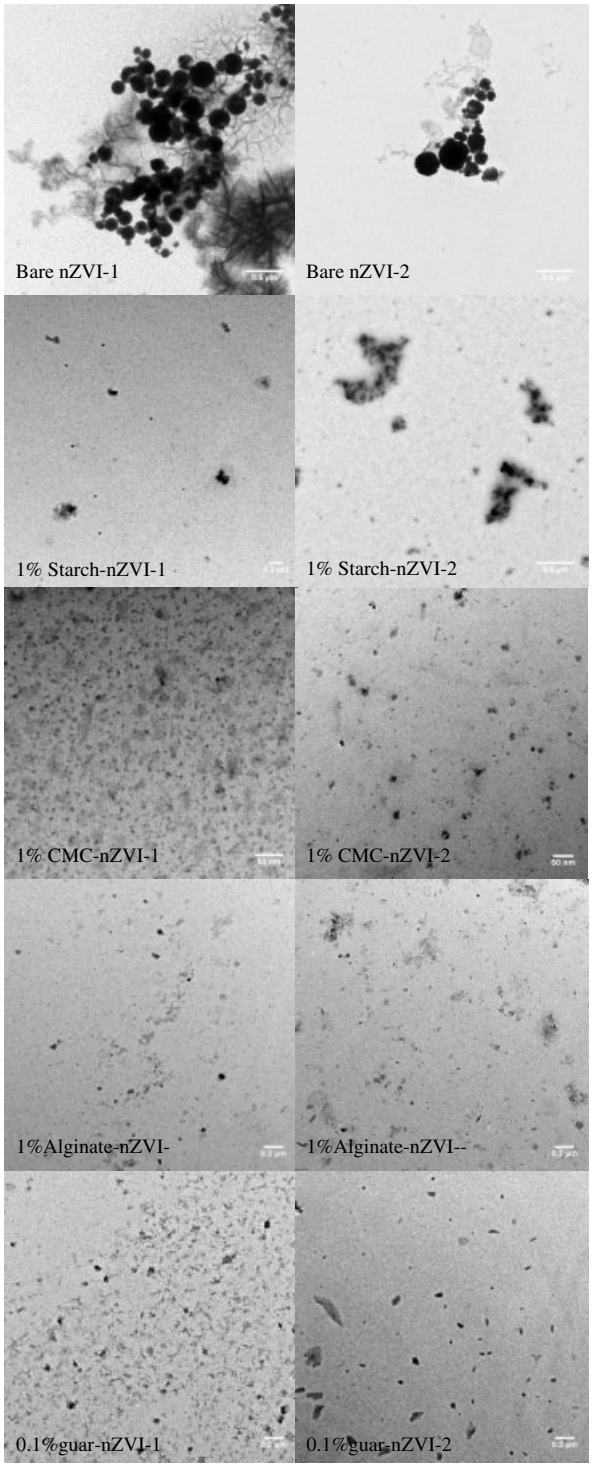

Figure 1. TEM image of bare nZVI and polymer-modified nZVI. 1 and 2 column represents fresh and 4 weeks aged sample. Iron concentration 0.2 g L^{-1}.

enclosed in clusters of approximate size 20–30 nm. These clusters are not homogeneously dispersed within a polymer film as was the case for the fresh CMC coated iron particles. The alginate coated nZVI particles showed similar size distribution to the CMC coated ones. This is probably due to the presence of carboxylate functional groups in both polymers, which are reported to complex Fe^{2+} hindering the crystal growth during synthesis and resulting in very small nanosized iron particles.[26] Even though the fresh alginate coated nZVI particles formed few clusters, the frequency and size of the clusters increased upon aging. Finally, the fresh guar gum coated iron particles appear enclosed in a very thick film of polymer with particle size of the order of a few nanometers. The particles appear enclosed in clusters less than 100 nm in diameter. It seems that upon aging for 4 weeks, the guar gum coated iron particles were enclosed in larger clusters than the fresh ones. The cluster size appears to increase from approximately 50–100 nm to approximately 100–200 nm. The large clusters formed upon aging for most polymer-coated nZVI particles may reduce the available surface area resulting in decreased reactivity.

Zeta potential results

Polymer induced particle stabilization usually includes steric stabilization and/or electrostatic repulsion for regular and aged samples. The unmodified nZVI registered negative zeta potential values around pH 7. This could be attributed to the formation of an hydroxylated FeO iron oxide layer (Table 1) as reported by Zhang *et al*.[27] The surface charge of the iron particles became significantly more negative upon coating with CMC or AA. This decrease is most likely due to the negatively charged carboxylate groups present in these two polymers. The CMC-nZVI and alginate-nZVI retained high negative surface charge over a 4-week period, indicating that CMC and alginate remained adsorbed to the nZVI surface and interface. The significant decrease in surface charge indicated that the electrostatic effect may play an important role in inhibiting aggregation, and thus reducing the adhesion coefficient between the iron nanoparticles.[13] The carboxylate groups in CMC with a pKa $\sim$ 4.3 are expected to be fully dissociated at pH above 7.[28] Similar behavior is expected for alginate. It is worth noting that alginate showed stronger positive correlation between polymer concentration and zeta potential values than CMC at similar pH values (Table 1). The 1% CMC–nZVI demonstrated zeta potential of −66.7 mV whereas the 0.1%CMC–nZVI registered zeta potential of −46.9 mV compared with 1%alginate–nZVI with zeta potential of −118.5 mV and 0.1% alginate–nZVI with −52.1 mV.

The starch-coated nZVI exhibited slight negative surface charge with values greater than those measured for the bare nZVI at similar aging times and pH values. This may indicate a lack or scarcity of negatively charged surface functional groups. Similarly, guar modified iron nanoparticles appear to be neutrally charged with slight negative zeta potential values. The relative stability of the surface charge for the starch coated nZVI and guar gum coated nZVI also indicated that these polymers remained adsorbed to the iron nanoparticles. The stabilization mechanism of the starch coated nZVI and guar gum nZVI is expected to be due to steric hinderance because of the particle neutral surface charge.[16]

Suspension behavior of iron nanoparticles upon aging

Pictures of suspensions of the bare and modified iron nanoparticles were documented up to 4 weeks (Fig. 2). These pictures serve as a visual aid to assess the stabilization efficiency of the various polymers. There are two interesting changes to monitor in these pictures: sedimentation evolution and sample color transition. First, the bare and starch-coated nZVI nanoparticles showed similar sedimentation behavior and no color change. The iron nanoparticles for both samples settled within minutes after synthesis. The 1% polymer–nZVI (except starch–nZVI) samples demonstrated a high degree of dispersion and kept the nZVI stabilized for at least 2 weeks. Suspension stability was consistent with others reported in the literature; for example, sand column tests indicated stable CMC modified nZVI suspension even after 8 months of aging.[29] For the 0.1% polymer–nZVI samples, guar gum indicated the best stabilization behavior. A small amount of guar–nZVI was still suspended up to 4 weeks whereas other polymer-coated nZVI settled to the bottom of the vials after 2 weeks. Second, all the nZVI samples except for the bare and starch-coated nZVI experienced color transition within a 4-week aging period. Bare–nZVI and starch–nZVI were initially dark black then cleared due to the rapid aggregation and deposition. AA–nZVI, CMC–nZVI and guar–nZVI samples initially exhibited jet black like color and then transitioned to different colors upon aging. There was no oxygen contamination because the vials were

Table 1. Summary of pH value and zeta potential of nonstablized nZVI and polymer-stabilized nZVI samples within 4 weeks of evaluation. Iron concentration 0.2 g L^{-1}

	nZVI		0.1%guar–nZVI		0.1%starch–nZVI		1%starch–nZVI	
	pH	ξ (mV)	pH	ξ (mV)	pH	ξ (mV)	pH	ξ (mV)
Fresh	6.72	-17.4 ± 4.6	7.93	-0.6 ± 0.1	7.19	-8.4 ± 0.5	7.4	-4.5 ± 0.2
Week1	7.19	-15.3 ± 1.3	7.97	-0.5 ± 0.1	7.07	-12.9 ± 1.2	7.34	-4.8 ± 0.5
Week2	6.95	-16.2 ± 1.1	7.86	-1.7 ± 0.6	7.34	-10.2 ± 2.9	7.6	-10.9 ± 1.4
Week4	7.19	-15.4 ± 1.4	7.89	-1.2 ± 0.1	7.02	-7.4 ± 1.2	7.73	-6.3 ± 0.7
	0.1%CMC-nZVI		1%CMC-nZVI		0.1%Alginate-nZVI		1%Alginate-nZVI	
	pH	ξ(mV)	pH	ξ(mV)	pH	ξ(mV)	pH	ξ(mV)
Fresh	7.96	-46.9 ± 1.4	8.19	-66.7 ± 3.3	8.03	-52.1 ± 2.5	8.2	-118.5 ± 3.3
Week1	8.27	-41.9 ± 0.8	8.5	-67.9 ± 1.8	8.26	-51.4 ± 2.9	8.3	-103.1 ± 13.2
Week2	8.35	-47.3 ± 1.3	8.26	-68.8 ± 4.6	8.25	-55.7 ± 3.6	7.87	-103.8 ± 16.1
Week4	7.79	-43.1 ± 1.0	8.34	-59.0 ± 3.2	8.2	-58.4 ± 0.5	8.13	-113.8 ± 7.3

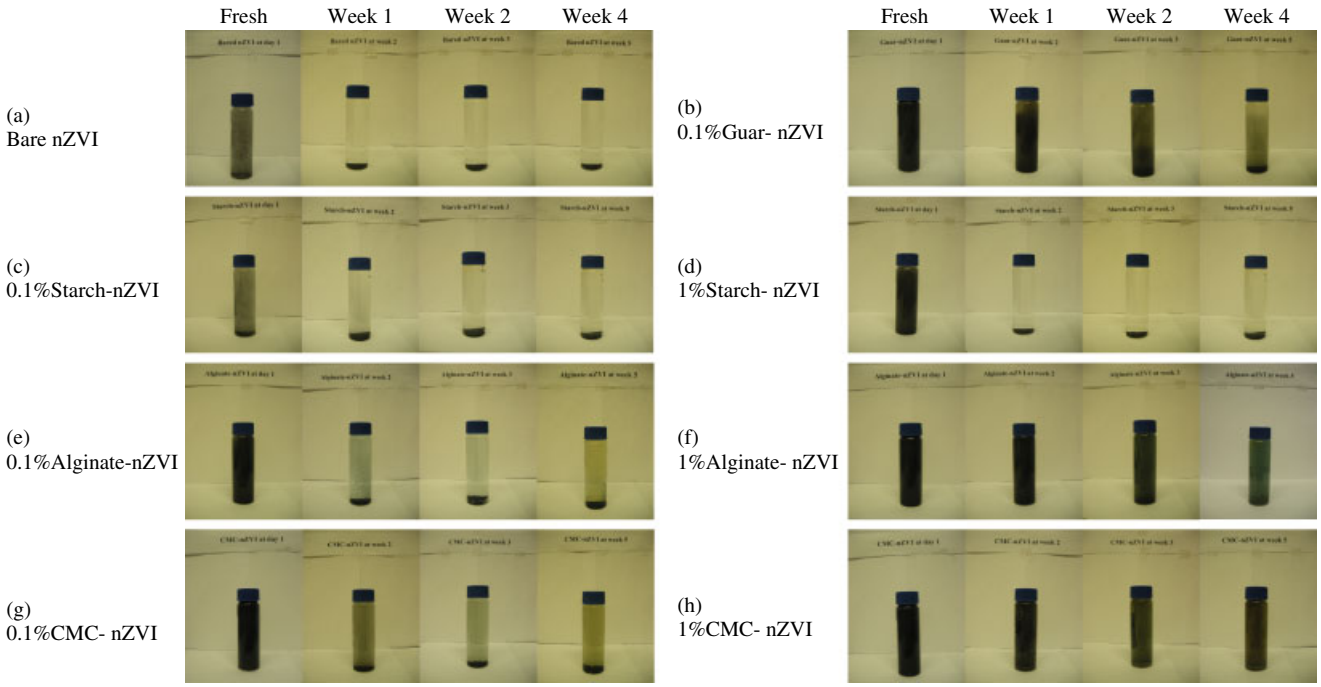

Figure 2. Suspension pictures taken at 0 min, 1 week, 2 weeks and 4 weeks. Iron concentration 0.2 g L^{-1} and no pH control: (a) bare nZVI, (b) 0.1%guar–nZVI, (c) 0.1%starch–nZVI, (d) 1%starch–nZVI, (e) 0.1%alginate–nZVI, (f) 1%alginate–nZVI, (g) 0.1%CMC–nZVI, (h) 1%CMC–nZVI.

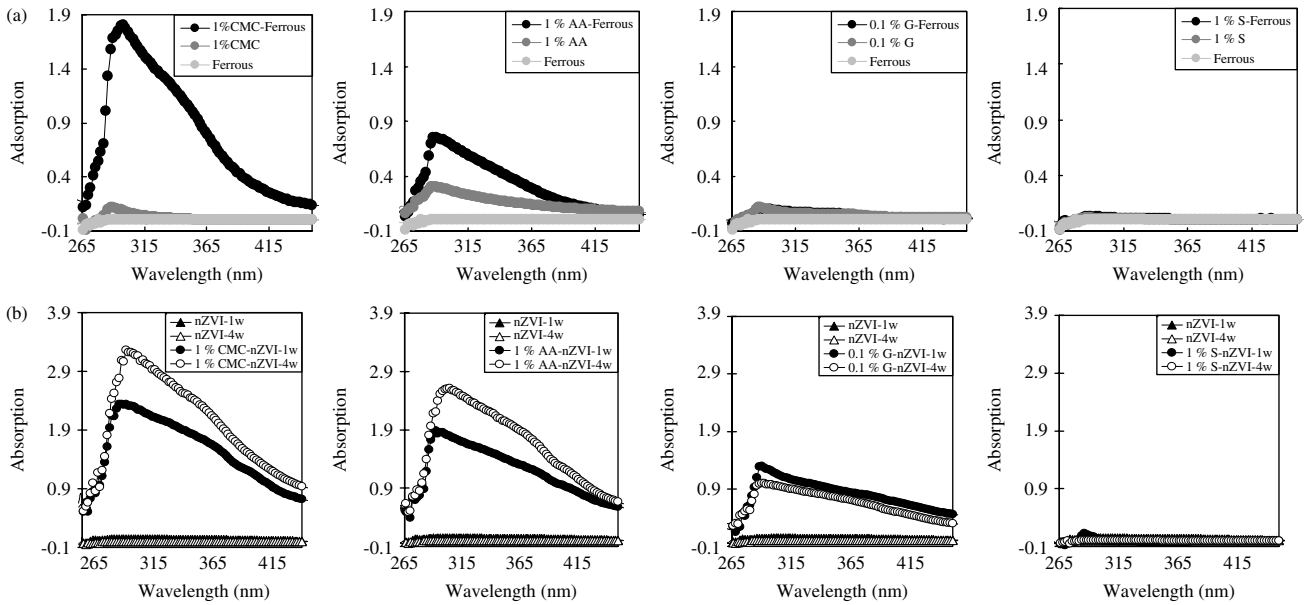

Figure 3. Absorption spectra of (a) polymer solution, ferrous solution and a solution containing polymer and ferrous (0.2 g L^{-1} Fe); (b) aged sample comparison. Polymer concentration at 1% (except 0.1% guar gum) and Fe^0 concentration at 0.2 g L^{-1}.

sealed and stored in a nitrogen glove box. Moreover, no color change was detected for the bare nZVI vials, which served as control. The color change of the CMC–nZVI sample from jet black to brown could be caused by complexation reactions between carboxylates and released ferrous.[26] Similarly, the AA–nZVI color change to green could indicate complexation reaction between AA and released ferrous. A similar but lighter color transition was observed for the 0.1%CMC–nZVI and 0.1%AA–nZVI samples. The 0.1% guar–nZVI displayed a dark black color at the early age and the particles gradually settled down thereafter.

UV-VIS measurements

UV-VIS measurements were taken for select iron suspension samples to assess iron-complex formation upon aging. Electrostatic attraction can stimulate chelating reactions between ferrous ions and negative polyelectrolytes. A monodente chelating interaction has been reported between the carboxylate group and the Fe nanoparticle[26] color change from clear to yellow observed in our experiments upon addition of the ferrous solution to CMC or alginate solutions. The results (Fig. 3(A)) indicate that the optical density of CMC–Fe(II) and AA–Fe(II) increased significantly

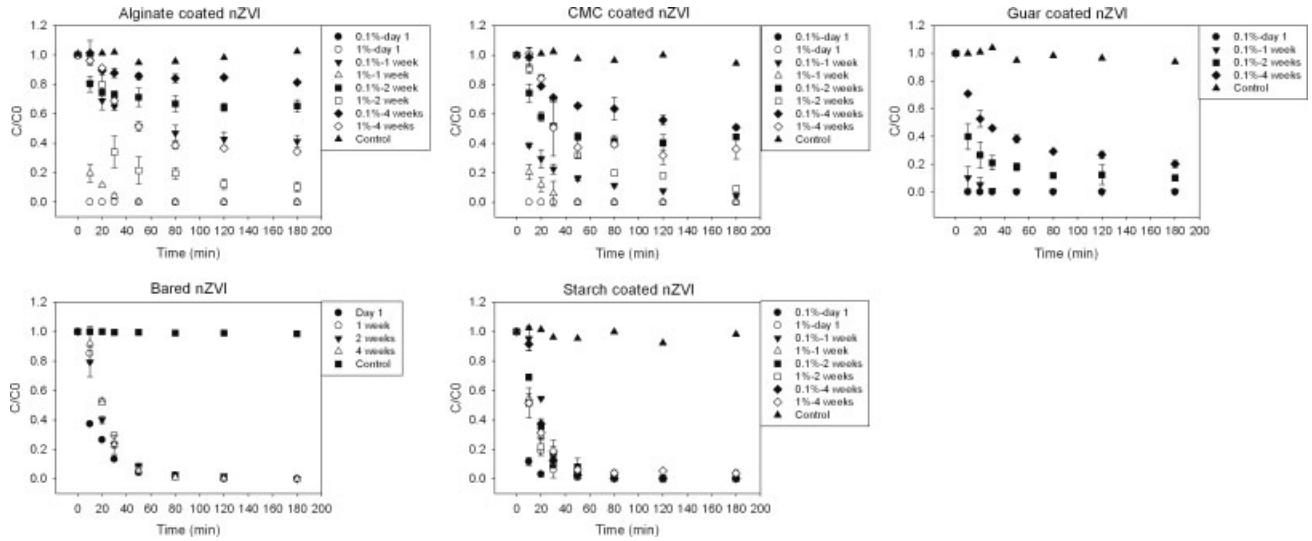

Figure 4. Degradation of RDX using bare iron and polymer-modified iron nanoparticles. All the tests were conducted with fresh, 1 week, 2 weeks and 4 weeks aged samples. Measurements were taken at 0, 10 min, 20 min, 30 min, 50 min, 80 min, 120 min and 180 min.

Table 2. Summary of estimated first-order kinetics rate constant (k1, min^{-1}) of nonstablized nZVI and polymer-stabilized nZVI samples within 4 weeks evaluation. Iron concentration 0.2 g L^{-1}

	nZVI	0.1%guar–nZVI	0.1%starch–nZVI	1%starch–nZVI
Fresh	0.0611 ± 0.0035		0.0655 ± 0.0185	0.0947 ± 0.0030
Week1	0.0516 ± 0.0034	0.1123 ± 0.0267	0.0814 ± 0.0096	0.0946 ± 0.0102
Week2	0.0502 ± 0.0028	0.0315 ± 0.0069	0.1301 ± 0.0133	0.079 ± 0.0043
Week4	0.0613 ± 0.0046	0.0187 ± 0.0023	0.0536 ± 0.0041	0.0556 ± 0.0030
	0.1%CMC–nZVI	1%CMC–nZVI	0.1%Alginate–nZVI	1%Alginate–nZVI
Fresh				
Week1	0.0332 ± 0.0053	0.1455 ± 0.0229	0.0126 ± 0.0012	0.1329 ± 0.0131
Week2	0.0156 ± 0.0022	0.0227 ± 0.0029	0.0006 ± 0.0015	0.0355 ± 0.0054
Week4	0.0089 ± 0.0011	0.0231 ± 0.0237	0.003 ± 0.0008	0.0142 ± 0.0015

compared with CMC, AA, or the ferrous solution spectra. A new shoulder appeared around wave number 340 nm indicating the presence of a CMC or alginate ferrous complex.[30] It is worth noting here that the intensity of the complex around wave number 340 nm increased upon aging (Fig. 3(B)) indicating an increase in the concentration of the Fe(II)–polymer complex. The aged 0.1%guar–nZVI sample did not exhibit an increase in the absorption probably due to weak complex formation.[31]

Degradation of RDX

Figure 4 shows time–concentration profiles for RDX degradation by nZVI. A pseudo-first-order reaction model was used to fit the RDX degradation data according to Equation (1):

$$-\frac{dC}{dt} = k_1 C \quad (1)$$

where C is the concentration of RDX (mg L^{-1}), t is time (min), and k_1 (min^{-1}) is the pseudo-first-order reaction rate. The RDX concentrations reached constant values within 80 min of contact with nZVI, hence, the first five sampling points were used to calculate the first-order constants k_1 (Table 2). In the presence of CMC, alginate and guar, the rate of RDX degradation by freshly modified nZVI (day 1) was rapid with complete removal of RDX achieved in less than 10 min, so the reaction rate values (k_1) for these experiments were not obtained.

It appears that the RDX degradation rates with bare nZVI and starch coated nZVI remained virtually constant with aging. The rates in our experiment appear on the same order of magnitude as those reported in the literature. For example, a k_1 value of 0.019 min^{-1} was reported for iron nanoparticles,[9] a value of 0.016 min^{-1},[23] and 0.095 min^{-1}[22] were reported, compared with an average k_1 value of 0.0611 min^{-1} in this study.

Even though starch has shown poor stabilization efficiency for iron suspension, the fresh 1% starch–nZVI has shown a higher RDX degradation rate constant than the bare one. This could be attributed to the smaller iron particle size. Although the starch-coated particles formed clusters and deposited on the bottom of the vials, the particle size of the iron particles within the gel network remained small as shown in the TEM image (Fig. 1). The gel clusters or aggregates most likely broke up upon mixing during the RDX degradation experiments.

The optimization of the molar ratio of polymer to nZVI was not the focus of our experiment. However, the higher polymer loading (1%) polymer-coated nZVI exhibited larger reaction rates than the lower polymer loading ones (0.1%). Fresh 1% CMC–nZVI

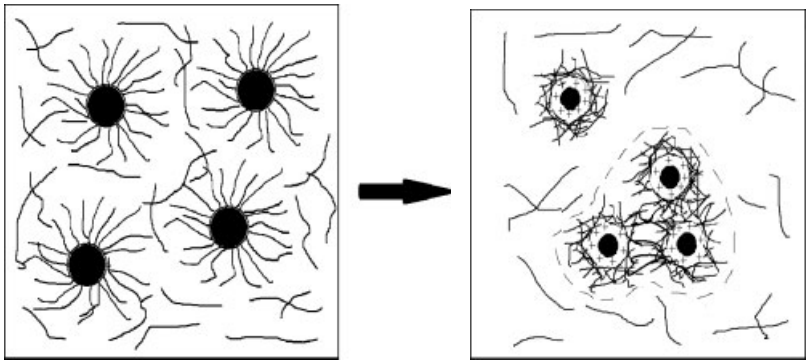

Figure 5. Schematic diagram of polymer conformation change with aging.

and 1% AA–nZVI produced the highest RDX degradation rate constant (0.13 min^{-1}) whereas 0.1% CMC–nZVI and 0.1%AA–nZIV attained rates approximately one order of magnitude lower. The 0.1%AA–nZVI attained a rate constant 3 times larger than the one attained by 0.1%CMC for all aging periods. The 4-week aged 1%CMC–nZVI and 1%AA–nZVI samples achieved a 65% RDX removal efficiency. The enhanced degradation rates at the higher polymer loading could be attributed to the formation of smaller iron particle size as reported by He *et al*.[26] They observed a significant decrease in iron particle size when the CMC/Fe ratio was increased.[32] Similarly, He *et al*.[33] reported faster TCE reduction rates by CMC-coated nZVI as CMC/Fe ratios increased.

Significant reduction in degradation rates was observed for the CMC and alginate coated iron nanoparticles upon aging. The decrease in degradation rates could be due to the formation of polymer-coated iron clusters, as shown in the TEM analyses. The formation of these clusters may obscure part of the iron surface thus reducing the number of available reactive sites. Upon aging, elemental iron can react with water releasing ferrous ions which potentially can complex with the negatively charged carboxylate groups of CMC and AA. The polymer–Fe^{2+} complexation can initiate bridging between various polymer-coated iron particles resulting in large clusters (Fig. 5).

Another possible mechanism contributing to the reactivity decrease includes polymer conformation change upon aging. For a highly concentrated polymer–nZVI suspension, the adsorption of polyelectrolytes to iron nanoparticles depends on the mass of the polyelectrolytes, the surface charge of solids and polyelectrolytes, the ionic strength, and temperature.[34] For constant ionic strength, polymer concentration, and temperature, surface charge has a dominant effect on polymer conformation at the iron surface. In this hypothesis, the released Fe^{2+} may adsorb to the iron surface hence attracting negative polymer chains (Fig. 5). The attracted chains tend to lay flat on the surface of the iron particles to neutralize the surface charge, similar to the train-loop-trail conformation model suggested by Scheutjens-Fleer.[34] Henrica *et al*.[35] reported that the amount of adsorbed polyelectrolytes varies linearly with the surface charge. Increasing the surface charge density leads to an increase in the adsorbed polymer to compensate for surface charge. Henrica *et al*.[36] verified the flat polymer conformation hypothesis using the volume fraction profile change of the polyelectrolytes. Theoretical calculations by Bohmer *et al*. showed that the adsorption of weak polyacid as a function of pH, showed that 80% of the polymer segments occur in trains at pH 8, indicating that highly charged polyelectrolytes lie essentially flat on the surface.[36] These conditions are similar to those in our aged CMC–nZVI (CMC $pK_a = 4.3$) and alginate–nZVI n ($pK_a = 2.95$ for carboxyl groups of alginic acid) systems, which support the flat polymer conformation hypothesis. Additional examples of the flat conformation of polyelectrolytes have been reported in the literature.[37,38]

The polymer conformation change could lead to blocking of the reactive sites at the Fe^0 surface, resulting in a reactivity decrease of the polymer-coated nZVI.[12,39] Even though the surface charge of the polymer-coated particle did not increase (more positive) upon aging contradicting the charge reversal hypothesis upon ferrous iron release, this concern could be discounted because of the high polymer density used in our study and the presence of excess adsorbed polymer at the iron surface. The lack of charge reversal was reported in other studies for CMC–nZVI and bare nZVI after 16 weeks aging.[29]

The 0.1% guar–nZVI exhibited RDX removal efficiency higher than the 1%CMC-modified nZVI and 1%AA-coated nZVI for similar aging periods. After aging for 1 month, the 0.1% guar-coated nZVI achieved 80% RDX degradation rate whereas the 1% CMC–nZVI and 1% alginate–nZVI samples achieved 65% RDX removal rates. Conversely, the 0.1% CMC–nZVI and 0.1% alginate–nZVI samples achieved 50% and 20% RDX removal rates, respectively. The higher RDX degradation efficiency achieved by the guar-coated nZVI could be due to the weaker guar–Fe^{2+} interaction than the CMC–Fe^{2+} or AA–Fe^{2+} interaction as there is only one lone electron pair from the oxygen atom in the guar hydroxyl group which could bind to Fe^{2+}.

CONCLUSIONS

Particle characterization, RDX degradation, and suspension stability experiments were used to assess the long-term dispersion of CMC-, alginate-, guar- and starch-coated nZVI, and the relative RDX degradation rates. Polymer modification resulted in smaller iron particle size and a potential gain in surface area. Hence, polymer-stabilized nZVI could achieve higher reactivity. However, upon aging, some of the reactive sites may be blocked resulting in reduced RDX diffusion rates to the particle surface. Site blockage is most likely caused by cluster formation and polyelectrolyte conformation change. An RDX degradation rate of 100% was achieved by the aged bare nZVI and starch-coated nZVI although these suspensions exhibited the least favorable dispersion behavior. Conversely, the aged CMC and AA samples achieved the best nZVI suspension stabilization but significantly lower RDX degradation rates at longer aging periods. Guar gum loading at one order of magnitude lower than CMC and AA achieved better RDX

degradation rates than both of these polymers, and maintained good dispersion at the same time. Guar gum is less subject to pH effects or interaction with ions encountered in the subsurface, which could result in reduced reaction efficiency. Based on the results of this study, guar gum, which is an economic biodegradable polymer, is highly suitable for *in situ* remediation. It is also demonstrated that, both migration and reactivity of polymer-stabilized nZVI should be explicitly evaluated over a long period before application in the field.

REFERENCES

1 Kaplan AS, Berghout CF and Pecznik A, Human intoxication from RDX. *Arch Environ Health* **10**:877–883 (1965).
2 Heilmann HM, Wiesmann U and Stenstrom MK, Kinetics of the alkaline hydrolysis of high explosives RDX and HMX in aqueous solution and adsorbed to activated carbon. *Environ Sci Technol* **30**:1485–1492 (1996).
3 Bose P, Glaze WH and Maddox DS, Degradation of RDX by various advanced oxidation processes: I. Reaction rates. *Water Res* **32**:997–1004 (1998).
4 Doong RA and Lai YJ, Dechlorination of tetrachloroethylene by palladized iron in the presence of humic acid. *Water Res* **39**:2309–2318 (2005).
5 Zhou H, Han J, Baig SA and Xu X, Dechlorination of 2,4-dichlorophenoxyacetic acid by sodium carboxymethyl cellulose-stabilized Pd/Fe nanoparticles. *J Hazard Mater* **198**:7–11 (2011).
6 Sun H, Wang L, Zhang R, Sui J and Xu G, Treatment of groundwater polluted by arsenic compounds by zero valent iron. *J Hazard Mater* **129**:297–303 (2006).
7 Bennett P, He F, Zhao D, Aiken B and Feldman L, *In situ* testing of metallic iron nanoparticle mobility and reactivity in a shallow granular aquifer. *J Contam Hydrol* **116**:35–46 (2010).
8 He F, Zhao DY and Paul C, Field assessment of carboxymethyl cellulose stabilized iron nanoparticles for *in situ* destruction of chlorinated solvents in source zones. *Water Res* **44**:2360–2370 (2010).
9 Naia G, Halasz A, Thiboutot S, Ampleman G and Hawari I, Degradation of dexahydro-1,3,5-trinitro-1,3,5-triazine (RDX) using zerovalent iron nanoparticles. *Environ Sci Technol* **42**:4364–4370 (2008).
10 McCormick NG, Cornell JH and Kaplan AM, Biodegradation of hexahydro-1,3,5-trinitro-1,3,5-triazine. *Appl Environ Microbiol* **42**:817–823 (1981).
11 Hoffsommer JC and Rosen JM, Hydrolysis of explosives in sea water. *Bull Environ Contam Toxicol* **10**:78–79 (1973).
12 Saleh N, Sirk K, Liu Y, Phenrat T, Dufour B, Matyjaszewski K, *et al*, Surface modifications enhance nanoiron transport and NAPL targeting in saturated porous media. *Environ Eng Sci* **24**:45–57 (2007).
13 Schrick B, Hydutsky BW, Blough JL and Mallouk TE, Delivery vehicles for zero valent metal nanoparticles in soil and groundwater. *Chem Mater* **16**:2187–2193 (2004).
14 Liu Y, Majetich SA, Tilton RD, Sholl DS and Lowry GV, TCE dechlorination rates, pathways, and efficiency of nanoscale Iron Particles with different properties. *Environ Sci Technol* **39**:1338–1345 (2005).
15 Comba S and Sethi R, Stabilization of highly concentrated suspensions of iron nanoparticles using shear-thinning gels of xanthan gum. *Water Res* **43**:3717–3726 (2009).
16 Tiraferri A, Chen KL, Sethi R and Elimelech M, Reduced aggregation and sedimentation of zero-valent iron nanoparticles in the presence of guar gum. *J Colloid Interf Sci* **324**:71–79 (2008).
17 He F and Zhao D, Preparation and characterization of a new class of starch-stabilized bimetallic nanoparticles for degradation of chlorinated hydrocarbons in water. *Environ Sci Technol* **39**:3314–3320 (2005).
18 BeMiller JN, Hydrocolloids, in *Gluten-Free Cereal Products and Beverages*, ed by Arendt EK and Bello FD. Elsevier Science Publisher, Burlington, pp. 203–215 (2008).
19 Wang J, Somasundaran P and Nagara JDR, Adsorption mechanism of guar gum at solid-liquid interfaces. *Miner Eng* **18**:77–81 (2005).
20 Biliaderis CG, Structures and phase transitions of starch polymers, in *Polysaccharide Association Structures in Food*, ed by Walter RH. Marcel-Dekker Inc, New York, pp. 57–68 (1998).
21 Yang H and Shen J, Dihydrazone of dialdehyde starch and its metal complexes. *Carbohy Polym* **56**:187–193 (2994).
22 Wanaratna P, Christodoulatos C and Sidhoum M, Kinetics of RDX degradation by zero-valent iron (ZVI). *J Hazard Mater* **136**:68–74 (2006).
23 Oh SY, Cha DK, Kim BJ and Chiu PC, Reductive transformation of hexahydro-1,3,5-trinitro-1,3,5-triazine, octahydro-1,3,5,7-tetranitro-1,3,5,7-tetrazocine, and methylenedinitramine with elemental iron. *Environ Toxicol Chem* **24**:2812–2819 (2005).
24 Gui L, Fenton HLR and Gillham RW, Degradation of RDX using granular iron and nickel-plated granular iron. *J Environ Sci Heal A* **44**:221–229 (2009).
25 Attard P, Antelmi D and Larson I, Comparison of the zeta potential with the diffuse layer potential from charge titration. *Langmuir* **16**:1542–1552 (2000).
26 He F, Zhao D, Liu J and Roberts CB, Stabilization of Fe-Pd nanoparticles with sodium carboxymethyl cellulose for enhanced transport and dechlorination of trichloroethylene in soil and groundwater. *Ind Eng Chem Res* **46**:29–34 (2007).
27 Sun Y, Li X, Cao J, Zhang W and Wang HP, Characterization of zero-valent iron nanoparticles. *Adv Colloid Interface* **120**:47–56 (2006).
28 Magdassi S, Bassa A, Vinetsky Y and Kamyshny A, Silver nanoparticles as pigments for water-based ink-jet inks. *Chem Mater* **15**:2208–2217 (2003).
29 Kim HJ, Phenrat T, Tilton R and Lowry G, Fe^0 nanoparticles remain mobile in porous media after aging due to slow desorption of polymeric surface modifiers. *Environ Sci Technol* **43**:3824–3830 (2009).
30 Mudasir , Yoshioka N and Inoue H, Ion paired chromatography of iron (II,III), nickel (II) and copper (II) as their 4,7-Diphenyl-1,10-phenanthroline chelates. *Talanta* **44**:1195–1202 (1997).
31 Abdel-Halim ES, El-Rafie MH and Al-Deyab SS, Polyacrylamide/guar gum graft copolymer for preparation of silver nanoparticles. *Carbohyd Polym* **85**:692–697 (2011).
32 He F and Zhao D, Manipulating the size and dispersibility of zerovalent iron nanoparticles by use of carboxymethyl cellulose stabilizers. *Environ Sci Technol* **41**:6216–6221 (2007).
33 He F and Zhao D, Hydrodechlorination of trichloroethene using stabilized Fe-Pd nanoparticles: reaction mechanism and effects of stabilizers, catalysts and reaction conditions. *Appl Catal B Environ* **84**:533–540 (2008).
34 Fleer GJ, CohenStuart MA, Scheutjens JMHM, Cosgrove T and Vincent B, *Polymers at Interfaces*, 1st edn. Chapman and Hall, London (1993).
35 Van de Steeg HGM, Cohen Stuart MA, de Keizer A and Bijsterbosch BH, Polyelectrolyte adsorption: a subtle balance of forces. *Langmuir* **8**:2538–2546 (1992).
36 Bohmer MR, Evers OA and Scheutjens JMHM, Weak polyelectrolytes between two surfaces: adsorption and stabilization. *Macromolecules* **23**:2288–2301 (1990).
37 Ferretti R, Zhang J and Buffle J, Kinetics of hematite aggregation by polyacrylic acid: effect of polymer molecular weights. *Colloid Surface A* **121**:203–215 (1997).
38 Gregory JJ, The effect of cationic polymers on the colloidal stability of latex particles. *J Colloid Interf Sci* **55**:35–44 (1976).
39 Phenrat T, Liu Y, Tilton RD and Lowry GV, Adsorbed polyelectrolyte coatings decrease Fe0 nanoparticle reactivity with TCE in water: conceptual model and mechanisms. *Environ Sci Technol* **43**:1507–1514 (2009).

